Volume 4
Number 2
March 2026
Pages 455-852

RSC Applied Polymers

rsc.li/RSCApplPolym

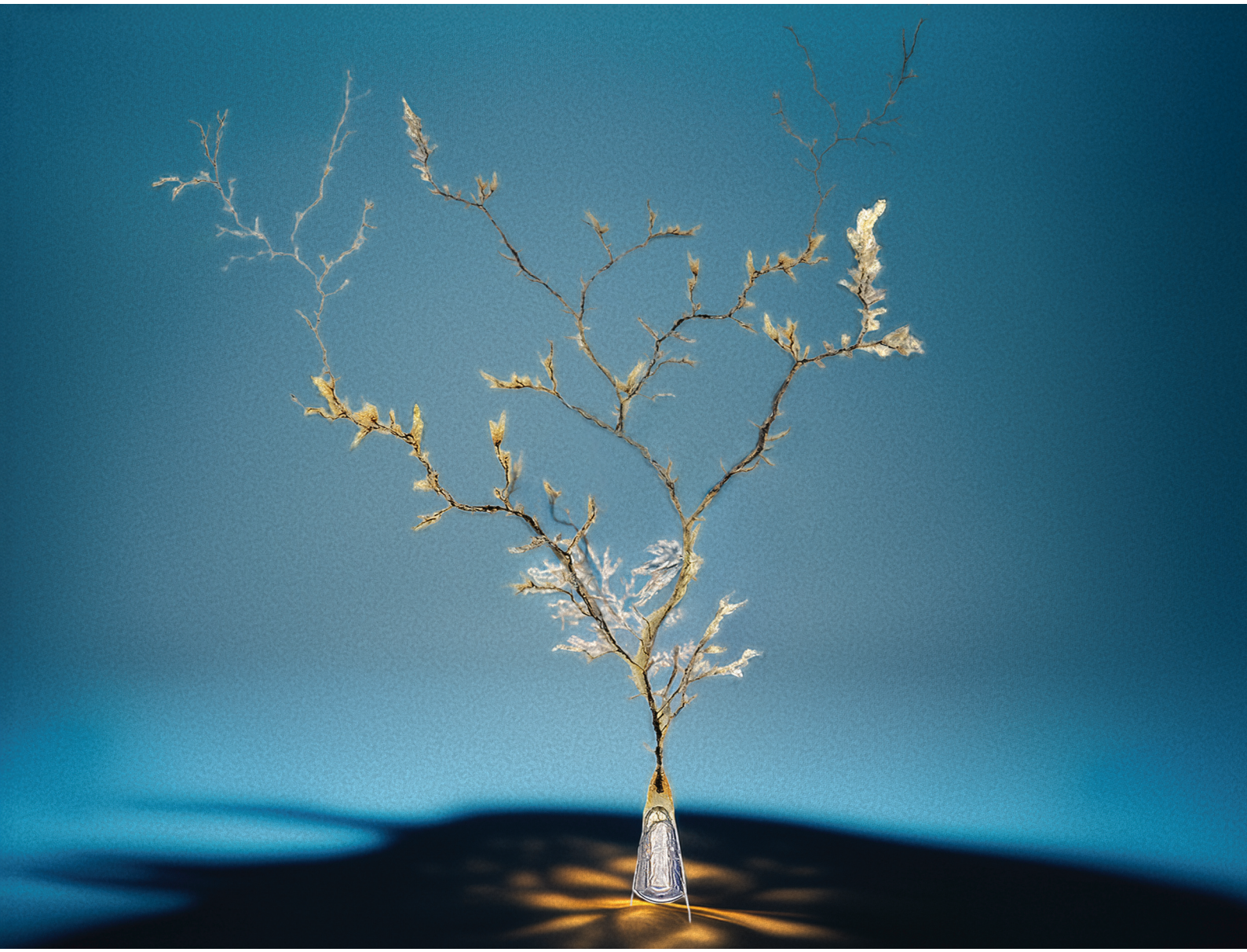

ISSN 2755-371X

ROYAL SOCIETY OF CHEMISTRY

PAPER
Henrik Strand, Mari-Ann Einarsrud *et al.*
Electrical treeing in stress-whitened polypropylene thermoplastic elastomer cable insulation

RSC Applied Polymers

ROYAL SOCIETY OF CHEMISTRY

PAPER

View Article Online
View Journal | View Issue

Cite this: *RSC Appl. Polym.*, 2026, **4**, 530

Electrical treeing in stress-whitened polypropylene thermoplastic elastomer cable insulation

Henrik Strand, *[a,b] Jorunn Hølto, [b] Sverre Hvidsten [b] and Mari-Ann Einarsrud *[a]

Polypropylene thermoplastic elastomer (PP-TPE) is emerging as an energy-saving and environmentally friendly alternative to cross-linked polyethylene (XLPE) for high-voltage cable insulation materials. However, the effect of mechanically induced stress whitening on electrical pre-breakdown of PP-TPE remains largely unexplored. This study investigates the influence of stress whitening generated by mechanical impact on electrical tree growth dynamics, morphology and associated partial discharge (PD) activity in extruded PP-TPE insulation taken from a commercially available cable. Electrical trees are initiated using a needle-plane configuration under AC voltage in samples with and without prior mechanical impact and thermal treatment. Impact-generated stress whitening is found to promote increased branching and alter growth directions, likely due to mechanical stress lines and localized material weakening, although it is not observed to significantly accelerate tree growth. Heating to sub-melt temperatures visibly reduces stress whitening but does not affect electrical treeing, suggesting that optical recovery does not reverse mechanical damage. Phase-resolved partial discharge analysis (PRPDA) reveals distinct PD patterns evolving through various phases of tree growth, with evidence of carbonization and gas pressure influencing PD dynamics.

Received 18th November 2025,
Accepted 15th January 2026

DOI: 10.1039/d5lp00365b

rsc.li/rscapplpolym

1. Introduction

Over the last two decades, polypropylene thermoplastic elastomer (PP-TPE) has received significant attention as a more environmentally friendly alternative to the conventional cross-linked polyethylene (XLPE) insulation system for power cables due to its smaller carbon footprint and recyclability.[1–3] Although XLPE has been the dominant material for electrical insulation of high voltage power cables since its introduction in the 1970s, several disadvantages of XLPE have been outlined, *e.g.*, limited recyclability due to its thermosetting characteristics and a long production cycle, resulting in high energy consumption.

Pure polypropylene (PP) cannot be used as cable insulation on its own due to its relatively high mechanical stiffness and brittleness, especially at low temperatures.[4] Therefore, one or several elastomers are added, either by copolymerization or blending, or a combination of the two. PP-elastomer blends have been studied since the 1980s and have a wide range of applications including in medical, automotive and packaging fields.[5–7] When used as cable insulation, PP-TPE constitutes a wide range of patented compounds developed by cable manufacturers. Their detailed compositions are not published but are likely based on a propylene-based homo- or copolymer matrix blended with a dispersed elastomeric phase, typically in the form of an ethylene- and α-olefin copolymer.[8,9] The compounds also contain additives such as dielectric liquids, antioxidants and UV stabilizers.

PP and its associated blends are known to exhibit macroscopic whitening when subjected to mechanical stress, such as tensile deformation or impact loading.[10–12] This phenomenon, known as stress whitening, arises from the formation of microcavities with sizes on the order of the wavelength of visible light (400–700 nm), leading to light scattering and a white appearance.[13] The cavities have been observed to occur under large strains (beyond the yield point), where the semicrystalline spherulitic structure of PP is destroyed and transformed into a fibrillar network through crazing, which upon further drawing breaks down and cavities are formed.[11,12] The initiation of such cavities at smaller strains (around the yield point) is believed to occur either in the interlamellar amorphous phase in the equatorial parts of the spherulites[13,14] or in the crystalline phase in the polar regions of the spherulites.[15] A unified model for cavitation in semicrystalline polymers combining these opposing views has been proposed.[16] For PP-elastomer blends, however, no such model has been reported in the literature. PP-elastomer blends are observed to

[a]*NTNU Norwegian University of Science and Technology, Trondheim, Norway. E-mail: mari-ann.einarsrud@ntnu.no, henrik.strand@sintef.no*
[b]*SINTEF Energy Research, Trondheim, Norway*

be more susceptible to stress whitening than pure PP, which has been ascribed to increased cavity formation at the boundaries between the PP and elastomer phases.[17]

Although stress whitening is reported to make the material more prone to diffusion of gases and liquids, reducing the mechanical strength and increasing the risk of fracture,[10] its impact on electrical treeing has, to the author's knowledge, not been reported in the literature. Nevertheless, recent studies have shown that even small tensile strains can significantly reduce the dielectric strength of PP-TPE, which is attributed to the formation of cavities in the nm range.[18] Stress-induced cavities in semicrystalline polymers have been found to nucleate in nm-sized pores in spaces adjacent to polymer chains,[19,20] and then to grow and even coalesce into larger ones under increasing strain.[21] This means that stress whitening could potentially include cavities that are large enough to serve as inception sites for partial discharges and electrical trees.[22]

Partial discharges (PDs) are localized dielectric breakdowns that occur in regions of high electric field stress such as cavities, inclusions or delaminations. The localized breakdown voltage inside a cavity depends on the type of gas it is filled with, the cavity size and the gas pressure.[22] The initial pressure in mechanically induced cavities is likely near vacuum.[23] Over time, gases such as oxygen and nitrogen dissolved in the polymer matrix may diffuse into these cavities, gradually increasing the internal pressure until reaching equilibrium.[24] Due to the lower permittivity of the gas compared to that of the polymer, the electric field inside the cavity is intensified.[22] If the voltage across the cavity exceeds the breakdown threshold, a discharge may occur. PDs release energy in the form of current impulses, heat, light and sound, degrading the cavity surface through various processes like chemical dissociation, ultraviolet radiation, electron and ion bombardment, and mechanical degradation from high-energy gases.[22] Over time, this may lead to tree-like degradation structures known as electrical trees.

Electrical treeing is a pre-breakdown phenomenon in polymeric insulation which consists of hollow interconnected gaseous tubules propagating through the material.[22] The growth of the tree will eventually lead to catastrophic failure when the branches bridge the insulation by reducing its dielectric strength. Electrical trees can initiate in regions with elevated electric field stress, such as cavities or protrusions, and propagate by erosion of the insulation through processes such as PD, autoxidation, penning ionization and/or electromechanical stress from increased gas pressure.[25,26] Several studies have found that electrical treeing is accelerated by tensile deformation,[27–32] and the dielectric breakdown strength of polyethylene-based insulation is found to decrease with mechanical strain from bending.[33,34] For composite insulation materials like PP-TPE, the growth of electrical trees has been observed to depend on the adhesion properties between the compound constituents,[26] as well as the crystalline morphology of the PP matrix.[35] Furthermore, the inclusion of an elastomeric phase in PP-TPE is reported to suppress electrical tree degradation under severe bending compared to that in pure PP samples.[36]

Nevertheless, the effect of the well-known stress whitening phenomenon on the electrical pre-breakdown of PP-TPE cable insulation is not reported. There is thus a major knowledge gap concerning the short- and long-term electrical degradation of such materials. Power cables are subjected to various types of mechanical stress during their lifetime, including pulling, bending and clamping, all of which could lead to stress whitening on surfaces and in the bulk of the insulation. Hence, the determination of the effect of stress whitening on electrical pre-breakdown is of utmost importance to avoid unexpected failures and outages.

In this work, we present the effect of mechanically induced stress whitening from impact on electrical treeing in an extruded PP-TPE cable insulation material. The initiation, growth dynamics and morphology of the electrical trees and their associated partial discharge activity are reported. Chemical analyses of electrical tree structures and scanning electron micrographs of stress-whitened PP-TPE are presented. A commercially available extruded cable rather than laboratory-moulded specimens was used to study the phenomena. This approach was selected to have an industrially relevant material in terms of composition, morphology, crystallinity and thermal history.

2. Experimental

2.1. Materials and sample preparation

The samples for electrical treeing measurements were taken from the insulation of a commercial 30 kV PP-TPE cable manufactured by Rosendahl Nextrom. The aluminium conductor of 15 mm diameter was removed, leaving an insulation system of 35 mm diameter, consisting of an 8 mm thick insulation layer with two semiconductive screens of 1 mm thickness (Fig. 1A and B). The insulation system was cut into discs of 3 mm thickness. Rectangular sections of 10 × 7 mm were punched out using a press knife, as shown in Fig. 1B. Part of the conductor screen was included in the rectangular sections to serve as the ground electrode for the electrical treeing experiments. The surfaces of the samples were polished to 2 mm thickness using a Struers LaboPol-30 wet polishing machine (Ballerup, Denmark) with #2000 SiC paper, followed by a 6 μm diamond polishing pad. A custom-made sample holder was used for the insertion of a 300 μm diameter stainless-steel needle with a tip radius of less than 2 μm. The sample was heated to 65 °C to soften the material[37] prior to manual insertion of the needle with the target of creating a 2 ± 0.1 mm gap from the conductor screen, as shown in Fig. 1C.

In total, four sets of samples with five specimens of each type were used for the treeing experiments, as summarized in Table 1. Set 1 consisted of untreated samples of PP-TPE insulation. In Sets 2 and 4, stress whitening was generated before needle insertion using an Instron CEAST 9350 drop tower impact system (Pianezza, Italy). A blunt striking head of 1 mm

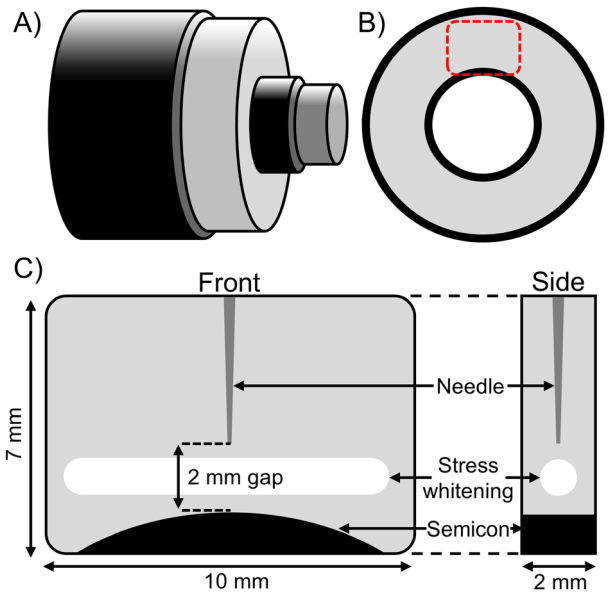

Fig. 1 (A) Cable core consisting of insulation, semiconductive screens and conductors; (B) disc of the cable insulation system, rectangular cut-out indicated by the dashed box; (C) front and side views of samples with a needle, stress-whitened area and semiconductive screen as the ground.

Table 1 Sample sets, short names and their mechanical and/or thermal treatment

Set	Sample type (short name)	Treatment
1	PP-TPE no treatment (PP)	No treatment. For reference.
2	PP-TPE stress whitened (PP SW)	Stress whitening from impact.
3	PP TPE heated (PP HT)	No stress whitening, heated (100 °C, 18 h).
4	PP-TPE stress whitened heated (PP SW HT)	Stress whitening from impact, heated (100 °C, 18 h).

diameter was mounted on a rod, with the falling mass and height adjusted to generate a horizontal band of stress whitening situated at the middle of the 2 mm gap between the needle and the semiconductor (Fig. 1C). The impact experiments resulted in a sample indent with a depth of approximately 0.5 mm, which was later removed by polishing the surrounding material, giving a stress-whitened region situated in the middle of the sample. The recorded impact data are presented in Table S1 and Fig. S1 in the SI. The applied mechanical impact methodology reflects practices recommended for assessing damage by mechanical impact in subsea cable systems.[38]

Sets 3 and 4 were heated to 100 °C for 18 hours. This is below the material's melting temperature of 155 °C, determined by differential scanning calorimetry. Set 4 initially exhibited stress whitening, which was optically reduced by more than 90% after heat treatment. This apparent reduction in stress whitening was estimated using the built-in pixel recognition tool of a Keyence VHX-X1 optical microscope (Osaka, Japan). These results are presented in Fig. S2 and S3 in the SI.

2.2. Experimental setup and electrical treeing procedure

The electrical treeing experiments were performed with a needle-plane geometry in the experimental setup shown in Fig. 2. The sample was mounted in a test cell filled with Wacker AK100 silicone oil to avoid surface flashover and spurious discharges on the polymer surface. High voltage was supplied by a 50 Hz 110 kV PD-free AC source. A coupling capacitor of 800 pF was connected in parallel to the sample and used to couple the signal to an MPD 600 PD measurement system from Omicron (Klaus, Austria). The setup was verified to be PD free up to 20 kV with a background noise level below 1 pC. The sample capacitance was measured in the range of 0.8–1.5 pF at 50 Hz using a PM6303 RCL meter from Fluke (Everett, WA, USA). A Cascade II 1024 CCD high-speed camera from Photometrics (Tucson, AZ, USA) equipped with a long-distance objective recorded the tree growth.

A small tree (<200 μm) was initiated following a predefined protocol prior to the tree growth experiments. The starting voltage was 5 kV which was increased by 1 kV every 5 min until tree initiation. If no tree had been initiated by 10 kV, the step duration was increased to 10 min. The tree initiation was manually detected using a camera and the PD signals.

The tree growth was performed at 11 kV. A 50 MΩ current-limiting resistor was placed between the high voltage source and the sample, as shown in Fig. 2, to protect the sample and setup in the case of breakdown. During tree growth, PD activity was continuously recorded, and images of the trees were captured every 12 s. The growth was continued until the tree bridged approximately 80% of the gap. For selected samples, tree growth was continued until breakdown.

2.3. Post-treeing analysis

The electrical trees were imaged using a Keyence VHX-X1 optical microscope (Osaka, Japan). For a detailed view of the tree morphologies, the samples were cut into 50–150 μm thick slices using an MT 990 motorized microtome from RMC Boeckeler (Tucson, USA) with a steel knife. Selected samples

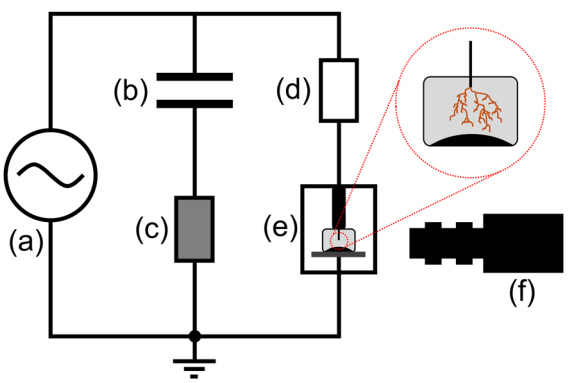

Fig. 2 Schematic of the experimental setup for electrical treeing. (a) High-voltage AC source, (b) coupling capacitor, (c) PD measurement unit, (d) current-limiting resistor, (e) test cell with electrodes and samples immersed in silicone oil, (f) CCD camera.

were prepared by cryo-ultramicrotomy using a Leica EM UC6/FC5 (Wetzlar, Germany) at −120 °C with a glass knife, producing very smooth surfaces in the stress-whitened regions. These were imaged by low vacuum scanning electron microscopy (LV-SEM) using the secondary electron detector of JEOL JSM-IT800 FE-SEM (Tokyo, Japan), operated at a pressure of 100 Pa.

The electrical tree channels were characterized by Raman spectroscopy using a WiTec Alpha 300R Raman spectroscope (Ulm, Germany). A monochromatic diode laser with a wavelength of 532 nm was utilized at a power of 0.5 mW, with a total of 100 accumulations and a 1 second integration time.

3. Results

3.1. Initiation and growth of electrical trees

Table 2 shows a summary of the electrical tree initiation and growth characteristics of all the samples. All trees initiated at voltages between 8 and 14 kV, with an average initiation voltage of 10.2 kV. The average initial tree length was 108 μm; however, as the voltage had to be manually shut off after initiation following optical and/or PD detection, the lengths of the initiated trees varied from 40 to 215 μm.

After the growth period, the final tree width, defined as the total horizontal spread of the tree, varied between 630 and 2090 μm, with an average of 1080 μm. The bridge gap time (*i.e.*, the time before approx. 80% of the gap was bridged) varied from 9 to 110 min, with an average of 37 min. The average growth rates (defined as the final vertical tree length divided by the total growth time) varied significantly between samples, with the slowest tree growing at an average rate of 16 μm min^{-1} and the fastest at 195 μm min^{-1}. The overall growth rates provide a limited view of the dynamics involved in the propagation of the electrical trees. Some samples exhibited phases of growth when the propagation nearly stopped completely for tens of minutes, followed by accelerated growth phases.

Fig. 3 shows the vertical growth of the trees as a function of time for the different sample sets. For Sets 1 and 3, where no stress whitening was introduced, two types of propagation dynamics were materialized: (i) continuous fast growth with rates between 100 and 195 μm min^{-1}, and (ii) three-phase growth with an initial fast growth of around 100 μm min^{-1}, followed by an intermediate plateau of around 5–10 μm min^{-1}, before a final acceleration to 100–150 μm min^{-1}. In Sets 2 and 4, which were both stress-whitened, similar patterns were observed, where some samples exhibited continuous fast growth at 80–150 μm min^{-1}, and others had slow phases of 5–20 μm min^{-1} before accelerating to 100–150 μm min^{-1}. Overall, the growth rates are comparable to those reported for unstressed XLPE under similar voltage levels and needle-plane gap distances, with average growth rates of 100 μm min^{-1}.[39,40]

3.2. Morphology of electrical trees

Fig. 4 shows typical tree morphologies for all sample sets, with photos captured during growth shown on the left and optical microscopy images of 150 μm thick microtomed slices shown on the right. In Fig. 4A and B, a clear distinction between slow-growing and fast-growing branches was observed. The slow growth was associated with a continuous expansion of existing tree branches, leading to wider channels (5–10 μm diameter), while the fast growth gave narrow channels (0.5–2 μm dia-

Table 2 Initiation properties (voltage, time and length) and growth characteristics (rate, time and width) of electrical trees in PP-TPE

			Initiation			Growth		
Set	Treatment	Sample name	Voltage (kV)	Time (min)	Initial tree length (μm)	Growth rate (μm min^{-1})	Bridge gap time (min)	Maximum tree width (μm)
1	No treatment	PP 1	10	35	100	93	19	1045
		PP 2	14	67	140	101	18	630
		PP 3	10	28	130	105	17[b]	1155
		PP 4	10	27	135	30[a]	67	1230
		PP 5	8	20	60	32[a]	55[b]	975
2	Stress whitened	PP SW 1	9	22	80	76	24	995
		PP SW 2	9	25	130	19[a]	99	990
		PP SW 3	8	18	60	49	39	975
		PP SW 4	10	26	120	149	12[b]	785
		PP SW 5	10	28	215	97	19[b]	1475
3	Heated	PP HT 1	12	48	120	37[a]	44	685
		PP HT 2	11	42	190	16	110	1515
		PP HT 3	13	55	50	35[a]	51	770
		PP HT 4	9	22	125	195	9	640
		PP HT 5	11	37	140	122	13	1510
4	Stress whitened heated	PP SW HT 1	11	38	115	73[a]	25	1675
		PP SW HT 2	10	25	80	136	14	635
		PP SW HT 3	9	25	40	50[a]	32	800
		PP SW HT 4	11	35	45	36[a]	47	2090
		PP SW HT 5	9	24	90	63	26	1010

[a] Highly variable growth rates during different phases of growth. See Fig. 3. [b] Retained at high voltage until breakdown.

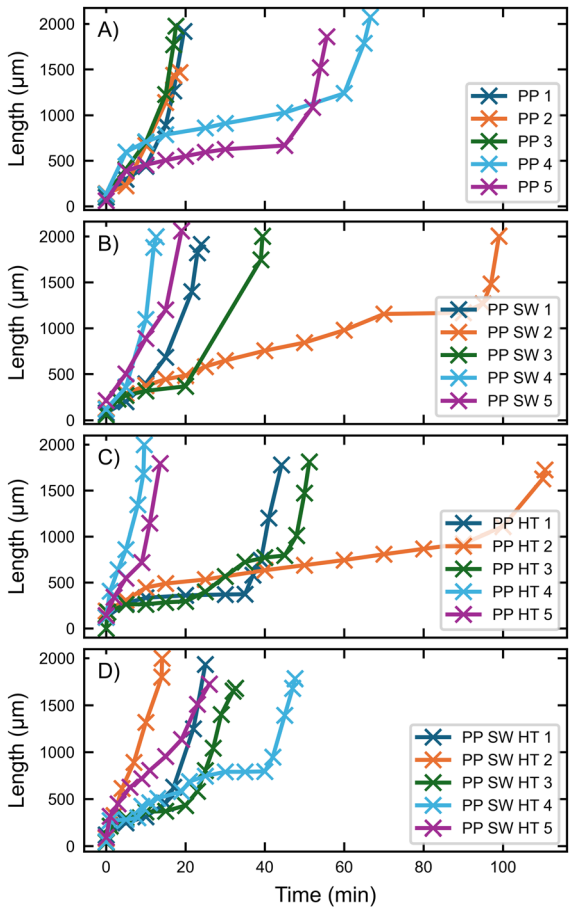

Fig. 3 Electrical tree propagation in (A) PP-TPE no treatment (Set 1); (B) PP-TPE stress whitened (Set 2); (C) PP-TPE heated (Set 3); (D) PP-TPE stress whitened heated (Set 4). Crosses are measurement points with linear estimation between.

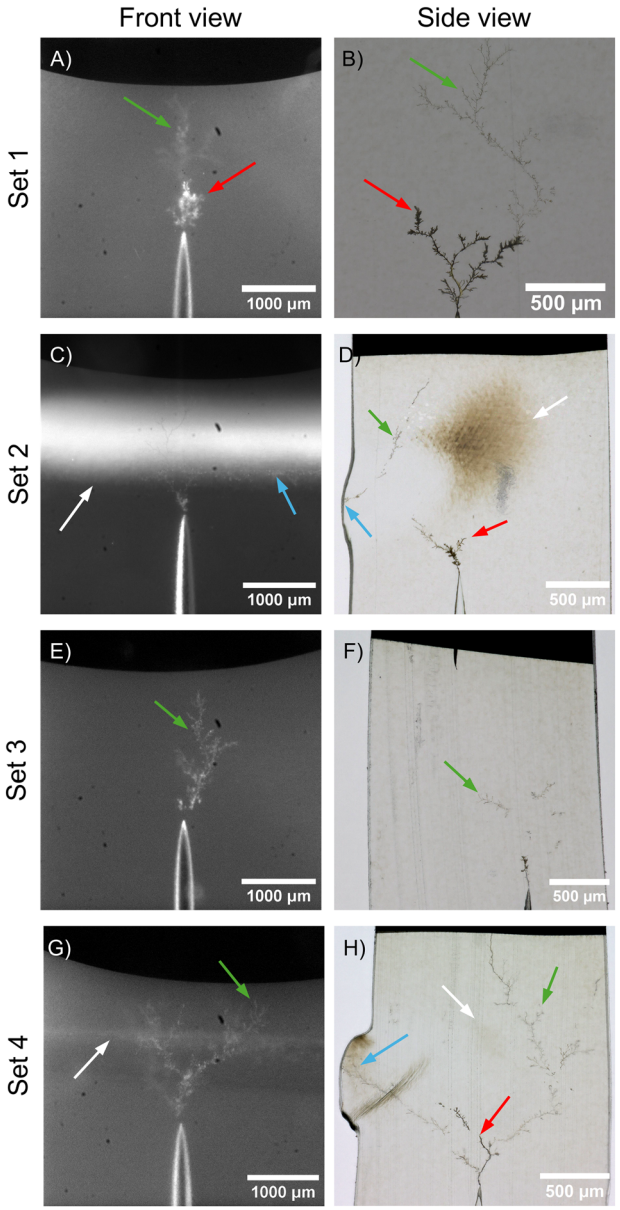

Fig. 4 Photos of typical electrical tree morphologies observed during growth (front view, left column – A, C, E and G) and optical microscopy images of microtomy-cut slices (side view, right column – B, D, F and H). Fig. 1C illustrates the difference between front and side views. Arrows indicate stress-whitened areas (white), thick branching (red), thin branching (green), and growth towards the impact zone (blue). The stress whitening appears brown in the optical images due to backlighting in the microscope.

meter). These observations are in accordance with previous studies, where slow vertical growth was associated with branched tree structures with wider channels, and fast growth with more bush-like trees with thinner channels.[35] One possible explanation for this is that the branching occurs when the energy associated with the discharge events at the tips of branches is not high enough to continue the growth of the present channel, but instead, erosion begins in a new channel in an adjacent weaker part of the material.[41]

In Sets 2 and 4, shown in Fig. 4C, D and G, H, a clear effect of mechanically induced stress whitening was observed. Several electrical trees exhibited preferential growth around the stress-whitened areas, which could be explained by an increase in density due to the compression during the impact events.[30] The trees tended to branch into wider structures when they reached the impact zone, with some branches preferentially growing towards the center of the impact zone, indicated by the blue arrows in Fig. 4C, D and H. This area was subjected to the highest mechanical stress, and the material had relaxed into a slight bump on the surface of the region of impact, which was even more prevalent in the heat-treated samples. Furthermore, some branches grew perpendicular to the electric field in the impact region near the surface of the sample, as indicated by the blue arrows in Fig. 4C and D.

The observed growth behaviour could be explained by the inclination of electrical trees to follow mechanical stress lines in pre-stressed insulation, with preferential growth occurring along mechanically weakened materials, *e.g.*, from tensile deformation.[42] Since the mechanical impact is associated with

a combination of tensile and compressive stresses, it can lead to a rather complex tensor of stress lines in the sample, as observed in the birefringence patterns shown in Fig. 5. The birefringence patterns are indicative of mechanical stress lines. The patterns observed in the unheated (Fig. 5A) and heated (Fig. 5B) samples are similar, indicating that the mechanical stress lines are preserved after heating, even though the visible stress whitening is reduced.

Fig. 6 shows the Raman spectra of an exposed electrical tree channel and a reference area outside the degraded region in sample PP 5. In the tree channel, two broad bands centred at around 1350 and 1580 cm^{-1} were observed, corresponding to the D and G bands of graphite, respectively.[43] This shows carbonization in the electrical tree channels, which has previously been proven to be the case for treeing in XLPE.[44] Furthermore, the progressively rising background signal is due to fluorescence, which also points to degradation or ageing of the specimen.[44] The reference spectrum exhibited several bands in 2800–3000 cm^{-1} attributed to the C–H vibrational modes in polypropylene, but no fluorescence was observed.

Fig. 7 shows an LV-SEM micrograph of an electrical tree channel in a stress-whitened region. The images of stress-whitened areas are interpreted as revealing interlamellar cracks within spherulites, with dimensions of around 0.5 μm, without destroying and transforming the spherulites into fibrils. The diameters of the propagating electrical tree branches were in the 5–10 μm range, much larger than the interlamellar cracks.

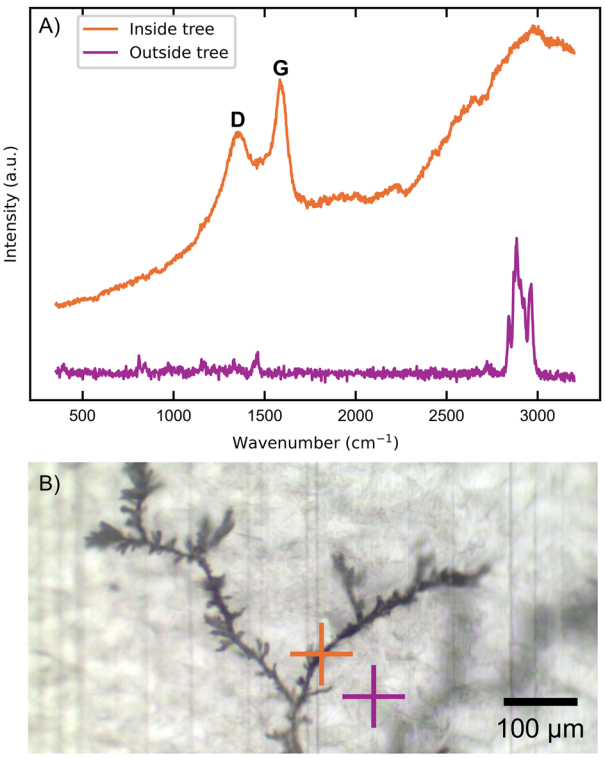

Fig. 6 (A) Raman spectra recorded inside a tree channel and outside the tree (reference location) in sample PP 5; (B) optical microscopy image with crosses showing the targeted regions where the spectra were recorded.

3.3. Treeing until breakdown

In the stress-whitened samples (Set 2) that were maintained at a high voltage of 11 kV until breakdown, a very high degree of branching was observed, as shown in Fig. 8A and B. In sample PP SW 4, the tree quickly bridged the gap after only 12 min, but hundreds of branches developed in the sample before finally breaking down after 94 min (Fig. 8B). The breakdown channel appeared to grow around the stress whitened area (Fig. 8C). This confirmed the observations in Fig. 4, where trees tended to grow around stress whitened areas. In sample PP SW 5, the tree bridged the gap after 19 min but was maintained at high voltage for the maximum experimental duration of 180 min without breaking down (Fig. 8A). The tree extended laterally towards the sample edges, resulting in a very wide tree of almost 10 mm. The samples without stress whitening exhibited much less branching before breakdown, as shown in Fig. 8D, which is consistent with previous observations for XLPE and fluoropolymers.[40] Studies on treeing in syndiotactic PP have reported extensive branching prior to breakdown.[45,46]

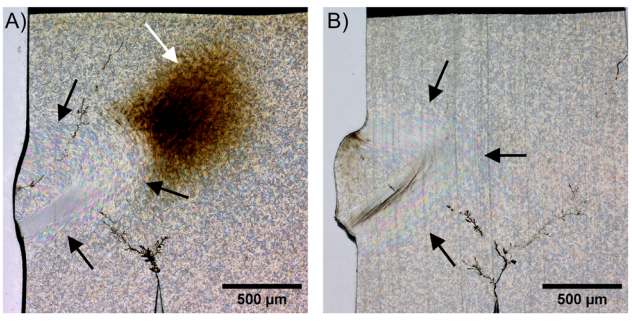

Fig. 5 Polarized optical microscopy images of birefringence interference patterns revealing mechanical stress lines in (A) a stress-whitened sample (Set 2) and (B) a stress-whitened heated sample (Set 4). Arrows indicate stress lines (black) and stress-whitened regions (white).

3.4. Partial discharges

Fig. 9 presents the evolution of PD activity during electrical tree growth in a stress-whitened sample (PP SW 2), characterized across three distinct growth phases: continuous, stagnation and runaway. The PD level and tree length increased concurrently during the continuous phase (0–70 min), with PD activity intensifying as the tree propagates (Fig. 9A). This increase was followed by a decline in PD level as the tree growth stagnated. In contrast, the PD energy, defined as the product of the applied voltage, discharge magnitude and discharge rate,[47] exhibited a steady increase throughout all phases of growth, followed by a sharp rise during the runaway phase (Fig. 9B). This shows that although the PD magnitude may decrease, the overall PD energy increases due to a higher PD rate during the final phase of tree growth.

The phase-resolved partial discharge analysis (PRPDA) plots associated with continuous growth, presented in Fig. 9C–E,

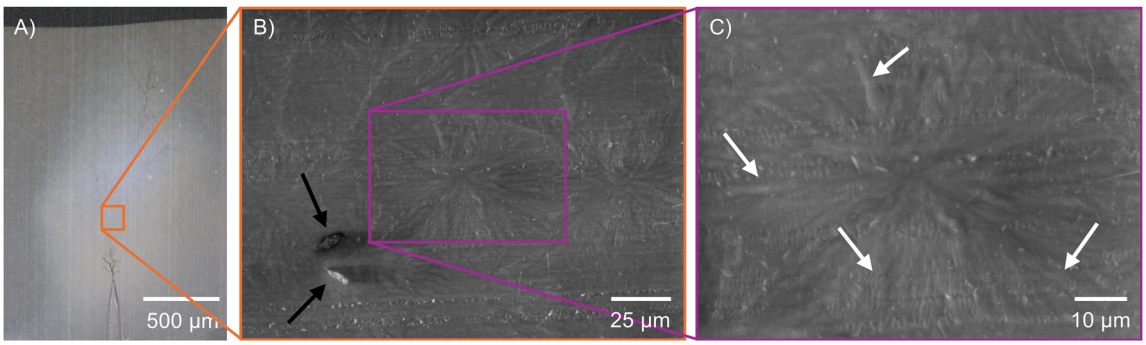

Fig. 7 (A) Optical image of an electrical tree in a stress-whitened area; (B) SEM micrograph of the stress-whitened area; (C) stress whitening-related cracks inside a spherulite. Arrows indicate branches of the electrical tree (black) and cavities (white).

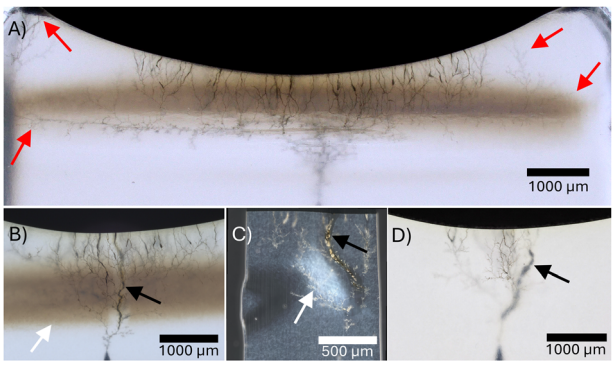

Fig. 8 Optical images of electrical treeing until breakdown in samples with (A, B and C) and without (D) stress whitening; (A) extreme branching without reaching breakdown, front view (PP SW 5); (B) breakdown in the stress-whitened region, front view (PP SW 4); (C) breakdown in the stress-whitened region, side view of a 150 μm microtomy slice (PP SW 4); (D) breakdown in an unstressed sample (PP 3). Arrows indicate the breakdown channel (black), stress-whitened area (white) and branching at extremities (red).

show wing-like patterns of increasing magnitude, which are typical for discharges along longer tree channels.[40,48] During the stagnation phase (70–90 min), the tree growth plateaued while the PD level gradually decreased from around 1000 pC to 600 pC. As shown in Fig. 9F–H, both the magnitude and shape of the PRPDA plots changed during this phase. The wing-like patterns gradually morphed into turtle-like patterns, indicating PD activity in shorter or partially carbonized channels.[48–51] This became even more pronounced during the runaway phase (95–99 min), where the tree growth accelerated rapidly while the PD magnitude decreased. However, the PD rate and PD energy increased strongly during late stagnation and runaway, indicating an increase in PD activity in the shorter channels.

Fig. 10 shows the typical temporal development of tree length, PD level, PD rate and PD energy for three growth rates: fast (PP SW HT 2), slow (PP HT 2) and mixed (PP 5). The fast-growing tree bridged the gap in less than 15 min, which was accompanied by an increase in PD level, PD rate and PD energy. The slow-growing tree had a slower continuous increase in PD level and PD energy, while the PD rate remained constant. The mixed-growth tree, however, showed an initial increase in PD level, before levelling off and decreasing when the growth plateaued, during which expansion of existing tree branches was observed (Fig. 4B). The PD rate fluctuated during the stagnation phase, before decreasing sharply during the runaway phase. This was also seen in the PD rate and PD energy, which decreased during the runaway phase, contrary to what was observed in stress-whitened material (Fig. 9B).

4. Discussion

4.1. Effect of stress whitening on electrical treeing

Mechanical pre-stressing and the generation of stress whitening in PP-TPE were observed to affect the morphology of electrical trees, leading to a higher degree of branching and different preferred growth directions than in unstressed material. This behaviour is ascribed to the electrical trees' tendency to follow mechanical stress lines, where growth is accelerated under tensile stress and decelerated under compressive stress.[30,42] Moreover, as PP-TPE is a composite insulation material, the treeing characteristics depend on the interfacial and adhesion properties between the PP and elastomeric domains and their interactions after mechanical pre-stressing.[26]

Since mechanical impact is associated with a combination of fast compressive, tensile and shear stresses, the resulting response consists of a mixture of linear elastic response, viscoplastic flow and non-linear strain-hardening elements.[52] The mechanisms involved in the formation of stress whitening by mechanical impact are thus not completely understood and have not been the main focus of interest in this paper. Nevertheless, the whitening is believed to be caused by scattering of visible light from cavities with dimensions around 0.5 μm. The cavities are much smaller than the diameter of the propagating tree branches, typically by a factor of 10. At such small cavity sizes, Paschen's law for breakdown in gas-filled cavities becomes increasingly inaccurate as the breakdown mechanisms deviate from the classical Townsend avalanche due to the limited ionization volume and the dominance of field emission and surface effects.[53] It has been

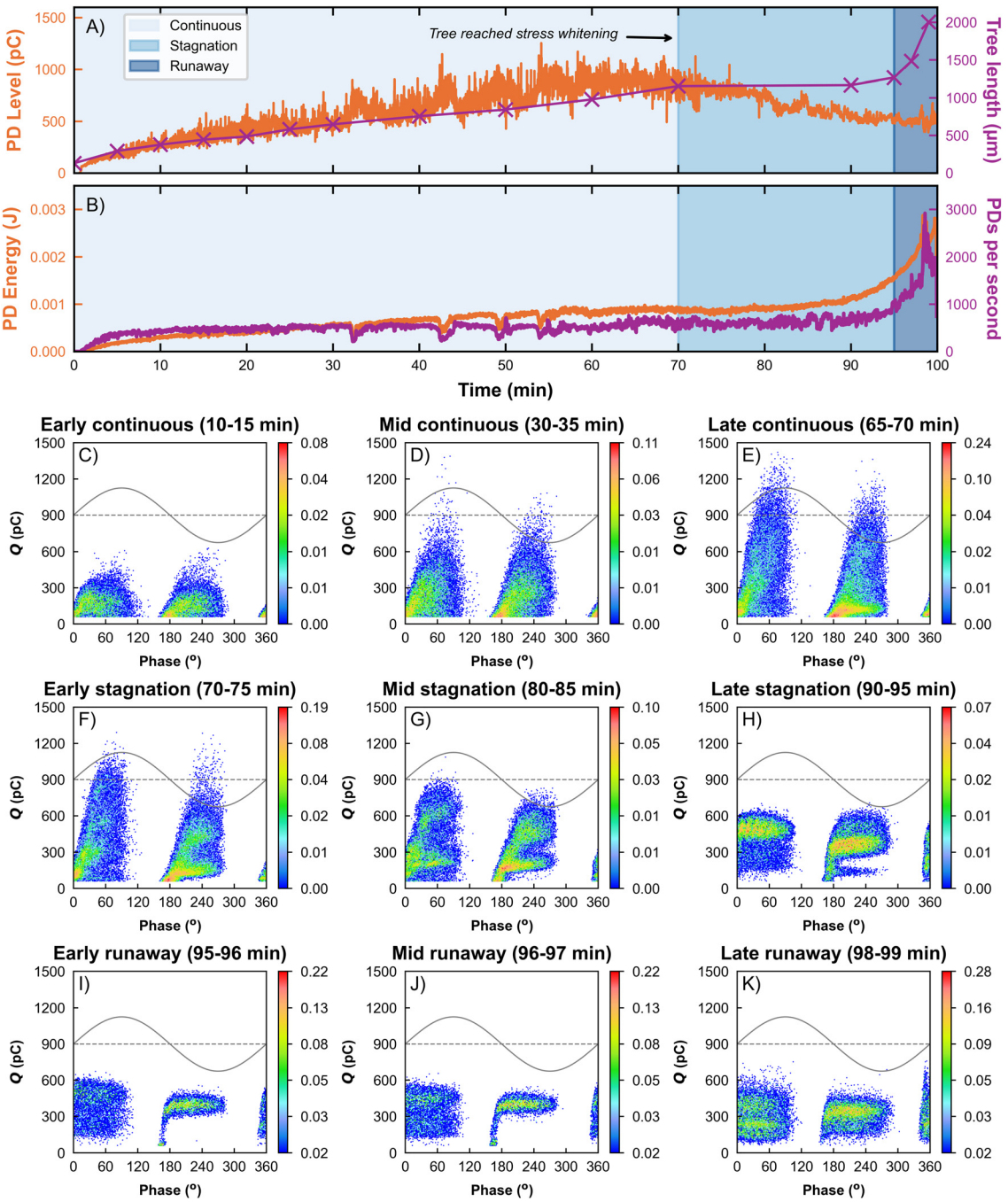

Fig. 9 (A) PD level and tree length during different phases of growth; (B) PD energy and the number of PD events over time; (C–K) associated PRPDA patterns during early, middle and late stages of continuous, stagnated and runaway growth phases, respectively. The colour bar indicates the number of PD events per second. All results are from sample "PP SW 2" from Set 2.

found that cavities below 1 µm in size do not impair the dielectric strength of solid insulation as they would require significantly higher electric fields to initiate discharges and the discharge magnitude tends to be lower.[54] This, in combination with the complex stress tensor and mechanical weakening of the material resulting from impact, could explain why no clear effect of stress whitening on the growth rates of electrical trees was observed.

Three distinct types of growth dynamics were identified in all sample sets: (i) slow growth, (ii) fast growth and (iii) mixed growth. During slow growth, the vertical growth of the trees stagnated or progressed very slowly; however, the existing branches continued to expand, leading to thick tree structures. Raman spectra (Fig. 6) confirmed that the thick branches were carbonized and degraded. Fast growth was associated with the formation of thinner tree branches with likely less carbonized

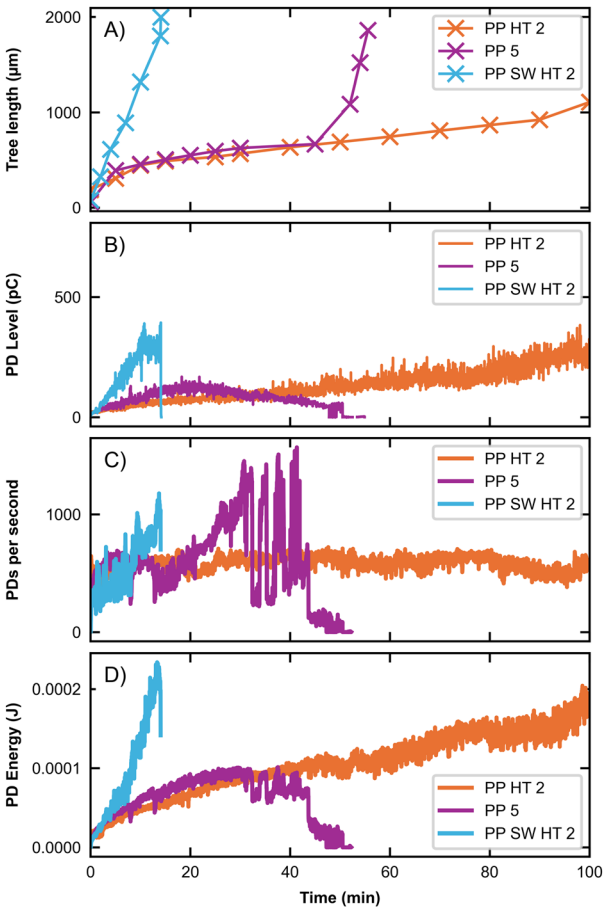

Fig. 10 (A) Tree length; (B) PD level; (C) PDs per second; (D) PD energy over time typical of fast (PP SW HT 2), slow (PP HT 2) and mixed (PP 5) tree growth rates.

volume. Mixed growth exhibited a combination of slow and fast periods. This is in accordance with previous findings[55] and can be explained by the inherently stochastic nature of electrical treeing, particularly since the local electric field strength varies as the tree propagates through the sample.[41,50] The observed growth rates and branched tree morphologies are consistent with results reported for unstressed XLPE tested under similar conditions. At 11 kV and a 2 mm gap distance, trees grown in XLPE were reported to exhibit branch-type structures with average growth rates of 103 µm min^{-1}.[39] Similar bush-branched morphologies were also observed in XLPE tested at 10 kV, with steady PD activity and 100 µm min^{-1} average growth rates.[40]

4.2. Apparent reduction of stress whitening

Although stress whitening was visibly reduced by heating, this had no clear effect on electrical treeing. The observed apparent reduction in whitening was possibly due to thermally induced local polymer chain rearrangements at sub-melt temperatures, enabling partial relaxation, shrinkage or closure of microcavities to sizes below the visible scattering range.[56] This would result in a less white appearance, even though the underlying mechanical damage and residual internal stresses by impact remain largely unchanged, as can be seen from the birefringence patterns in Fig. 5. This interpretation is supported by the similar tree morphologies and preferred growth directions observed in Sets 2 and 4, both of which were stress-whitened from mechanical impact, but only the latter was subjected to thermal treatment. The lack of change in treeing behaviour suggests that while heating may reduce the optical signature of the damage, it does not necessarily remove the internal stresses or defects that are relevant to electrical degradation.

4.3. Interpretation of the PD patterns

The interpretation of PD data from electrical treeing involves a complex interplay between various factors, notably cavity size and geometry, internal pressure, local electric field variations and space charge accumulation, as well as material degradation from mechanical cracking, carbonization and localized heating and remelting of tree channels.[22] During tree propagation in stress-whitened material, an evolution in PD level, PD energy and PRPDA, from wing-like to turtle-like patterns, was observed across different phases of growth, as shown in Fig. 9.

The detection of both wing-like and turtle-like PRPDA patterns during electrical treeing has previously been reported in several studies.[40,41,49–51,57] Lv *et al.* studied treeing in epoxy resin, and attributed the wing-like PDs to discharges in long channels, travelling the full length of the tree, and turtle-like patterns with PDs within short branches or at the tree tips.[49] These findings are in accordance with observations by Wu *et al.*, who proposed a similar explanatory model for treeing in low-density polyethylene.[57] The PRPDA data for continuous growth (Fig. 9C–E) support this model, exhibiting wing-like patterns of increasing magnitude as the tree grows. However, this does not explain why the PD level in sample PP 5 decreased as growth stagnated and continued to decrease even as the growth accelerated during the runaway, producing turtle-like patterns of low magnitude even for long trees.

A proposed explanation for the observed evolution in PD activity during stagnation and runaway is related to the conductivity of the tree channels.[41,50] As growth stagnates, the existing branches expand by material erosion and carbonization of the channel walls, turning them conductive. This effectively moves the front of the electric field from the needle closer to the tips of the tree, generating smaller discharges over shorter distances and resulting in turtle-like PD patterns. An alternative explanation may involve increased gas pressure forming within the tree channels, which has been observed to suppress PD by raising the local breakdown voltage during electrical treeing.[58] Supporting this, Fig. 11 shows that the main branches connected to the needle tip appear darkened, suggesting carbonization, while the branch tips appear lighter, exhibiting a cracked morphology, potentially indicative of localized rupture caused by elevated internal gas pressure during propagation.

The PRPDA plots associated with early and mid-runaway, shown in Fig. 9I and J, show a flat cluster of PDs of around 500

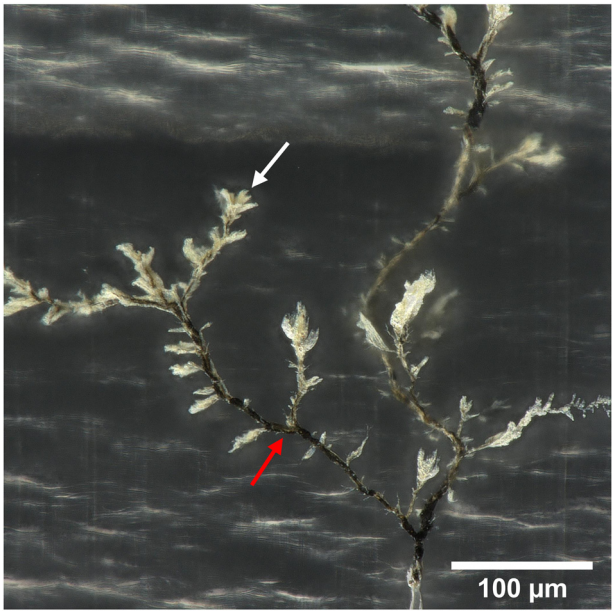

Fig. 11 Optical microscopy image of a 50 µm microtomy slice showing a typical slow-growing tree morphology in PP-TPE. Arrows indicate darkened carbonized channels (red) and cracked morphology at tips (white).

pC from 180° to 270° phase angle, *i.e.*, in the negative voltage half-cycle, while the cluster in the positive half-cycle was taller and distributed over a wider range of PD magnitudes. The observed asymmetry with respect to voltage may be due to polarity-dependent space-charge effects or changes in the local electric field caused by the evolving tree structure.[59] The fact that the cluster in the negative half-cycle appears to be floating is indicative of discharges originating from a floating potential, *e.g.*, a conductive inclusion.[60] Here, this may signify that the partially conductive channels formed during tree growth act as temporarily floating electrodes embedded in the polymer, possibly due to the melting of the PP-TPE creating discontinuous conductive channels.

The chemical degradation caused by PD can lead to the formation of acidic byproducts such as nitric or carboxylic acids, which in turn may influence the local dielectric properties and increase the conductivity of the channels, changing the PD dynamics.[61] This may explain why no reduction in PD activity was observed in the fast-growing trees (Fig. 10). These trees generally had narrower channels, possibly with less carbonization and chemical degradation, and hence lower conductivity. This would allow PDs to occur along the total tree length during the entire phase of growth.

4.4. Future prospects

The present study offers insights into electrical tree growth in PP-TPE insulation subjected to mechanical impact, with relevance to the reliability of power cable systems. The applied mechanical impact reflects recommended industry practices for mechanical testing of subsea cable systems.[38] Although stress whitening induced by impact was shown to affect tree morphology, no significant acceleration in tree growth or evidence of catastrophic dielectric failure was observed. Nevertheless, several questions remain open to future investigations. The current experimental setup did not allow for assessment of tree initiation and PD inception within stress-whitened regions, which is worth exploring further. Investigating the temperature dependence of stress whitening in PP-TPE, both at high and low temperatures, also warrants further analysis. Additionally, the effects of stress whitening arising from other mechanical actions, such as bending or peeling during the preparation of cable joints or terminations, may be especially relevant in practical applications. Applying stress whitening in other directions relative to the needle-plane gap, *e.g.*, in parallel or with spherical shape, could help separate the effects of mechanical stress lines from cavity formation on electrical tree dynamics. It should be noted that since PP-TPE compounds are proprietary and vary by manufacturer, the results presented in this work apply to the tested formulation. Future studies should include other PP-TPE variants to improve generalizability.

5. Conclusions

Stress whitening, caused by mechanical impact, was found to influence the morphology of electrical trees in a PP-TPE cable insulation material by promoting branching and altering preferred growth directions. However, stress whitening did not accelerate tree propagation or lead to severe degradation. Heating to sub-melt temperatures visibly reduced the whitening without affecting electrical treeing, suggesting that apparent optical recovery may not correspond to true healing of the material's underlying mechanical degradation following impact. PD activity was found to vary between different phases of growth (continuous, stagnation and runaway), as well as between different growth rates (fast, slow and mixed). The evolution of PD patterns appears to be governed by a combination of tree length, conductivity of channel walls, and internal gas pressure. Raman spectroscopy confirmed the presence of conductive byproducts such as graphite in slowly eroded channels, supporting the hypothesis that increased conductivity alters growth and PD dynamics.

Author contributions

Henrik Strand: data curation (lead), formal analysis (lead), investigation (lead), methodology (equal), funding acquisition (supporting), visualization (lead), and writing – original draft (lead). Jorunn Hølto: conceptualization (equal), project administration (lead), funding acquisition (equal), methodology (equal), supervision (supporting), and writing – review and editing (equal). Sverre Hvidsten: conceptualization (equal), funding acquisition (equal), methodology (equal), resources (lead), supervision (supporting), and writing – review and

editing (equal). Mari-Ann Einarsrud: conceptualization (equal), methodology (equal), funding acquisition (supporting), project administration (supporting), supervision (lead), and writing – review and editing (lead).

Conflicts of interest

The authors declare no conflicts of interest.

Data availability

Data for this article, including raw files from the different experiments, are available at Zenodo (https://doi.org/10.5281/zenodo.18174679).

Supplementary information (SI): results from the drop tower impact experiments and the heating experiments. See DOI: https://doi.org/10.1039/d5lp00365b.

Acknowledgements

This work was performed as part of the collaborative and knowledge-building project REWARD (project number 344481), funded in part by the Research Council of Norway and industry. The authors acknowledge Rosendahl Nextrom for providing the cable used in the experiments. We also thank M.Sc. Sofie B. Hårberg for performing the cryo-ultramicrotomy at the Cellular and Molecular Imaging Core Facility (CMIC) at NTNU and M.Sc. Andreas Grønbech for assisting in developing the heat treatment protocol to reduce stress whitening.

References

1 X. Huang, J. Zhang, P. Jiang and T. Tanaka, Material progress toward recyclable insulation of power cables part 2: Polypropylene-based thermoplastic materials, *IEEE Electr. Insul. Mag.*, 2020, **36**, 8–18.
2 Y. Zhou, S. Hu, C. Yuan, J. Hu, Q. Li and J. He, Recyclable polypropylene-based insulation materials for HVDC cables: Progress and perspective, *CSEE J. Power Energy Syst.*, 2020, **10**, 2208–2220.
3 J. Li, K. Yang, K. Wu, Z. Jing and J.-Y. Dong, Eco–friendly polypropylene power cable insulation: Present status and perspective, *IET Nanodielectr.*, 2023, **6**, 130–146.
4 W. Grellmann, S. Seidler, K. Jung and I. Kotter, Crack-Resistance Behavior of Polypropylene Copolymers, *J. Appl. Polym. Sci.*, 2001, **79**, 2317–2325.
5 B. Z. Jang, D. R. Uhlmann and J. B. V. Sande, Crystalline morphology of polypropylene and rubber–modified polypropylene, *J. Appl. Polym. Sci.*, 1984, **29**, 4377–4393.
6 B. Z. Jang, D. R. Uhlmann and J. B. V. Sande, Rubber–toughening in polypropylene, *J. Appl. Polym. Sci.*, 1985, **30**, 2485–2504.
7 *Handbook of polypropylene and polypropylene composites*, ed. H. G. Karian, Marcel Dekker, New York, 2003.
8 Prysmian SpA, *World Intellectual Property Organization*, WO2013/017916A1, 2013.
9 Nexans, *U.S. Patent and Trademark Office*, 11525050B2, 2022.
10 S. Bakshi, A. K. Kulshreshtha, B. P. Singh and J. S. Anand, Stress-whitening of polypropylene block copolymer in impact tests and its measurement, *Polym. Test.*, 1988, **8**, 191–199.
11 Y. Liu and R. W. Truss, A study of tensile yielding of isotactic polypropylene, *J. Polym. Sci., Part B: Polym. Phys.*, 1994, **32**, 2037–2047.
12 Y. Liu, C. H. L. Kennard, R. W. Truss and N. J. Calos, Characterization of stress-whitening of tensile yielded isotactic polypropylene, *Polymer*, 1997, **38**, 2797–2805.
13 A. Pawlak, A. Galeski and A. Rozanski, Cavitation during deformation of semicrystalline polymers, *Prog. Polym. Sci.*, 2014, **39**, 921–958.
14 A. Pawlak and A. Galeski, Cavitation during tensile deformation of polypropylene, *Macromolecules*, 2008, **41**, 2839–2851.
15 Y. Men, J. Rieger and J. Homeyer, Synchrotron ultrasmall-angle X-ray scattering studies on tensile deformation of poly (1-butene), *Macromolecules*, 2004, **37**, 9481–9488.
16 Y. Lu and Y. Men, Cavitation-induced stress whitening in semi-crystalline polymers, *Macromol. Mater. Eng.*, 2018, **303**, 1800203.
17 Y. Lu, Y. Sun, L. Li and Y. Men, Influence of propylene–based elastomer on stress–whitening for impact copolymer, *J. Appl. Polym. Sci.*, 2017, **134**, app.44747.
18 K. Wu, H. Sui, Q. Qi, Z. Yang, P. Zhao, Y. Qin, K. Yang, B. Ouyang, S. Li and J. Li, Small Strain-Induced Abrupt Drop in the Electrical Breakdown Strength of Polypropylene Insulation, *Nano Lett.*, 2025, **25**, 16270–16277.
19 A. Rozanski and A. Galeski, Plastic yielding of semicrystalline polymers affected by amorphous phase, *Int. J. Plast.*, 2013, **41**, 14–29.
20 A. Rozanski, A. Krajenta, R. Idczak and A. Galeski, Physical state of the amorphous phase of polypropylene-influence on free volume and cavitation phenomenon, *J. Polym. Sci., Part B: Polym. Phys.*, 2016, **54**, 531–543.
21 C. Thomas, V. Ferreiro, G. Coulon and R. Seguela, In situ AFM investigation of crazing in polybutene spherulites under tensile drawing, *Polymer*, 2007, **48**, 6041–6048.
22 L. A. Dissado and J. C. Fothergill, *Electrical degradation and breakdown in polymers*, IET, 1992, vol. 9.
23 A. Gałeski and E. Piórkowska, Localized volume deficiencies as an effect of spherulite growth. II. The three-dimensional case, *J. Polym. Sci., Polym. Phys. Ed.*, 1983, **21**, 1313–1322.
24 B. Duncan, J. Urquhart and S. Roberts, *Review of Measurement and Modelling of Permeation and Diffusion in Polymers*, 2005.
25 X. Zheng and G. Chen, Propagation mechanism of electrical tree in XLPE cable insulation by investigating a double

electrical tree structure, *IEEE Trans. Dielectr. Electr. Insul.*, 2008, **15**, 800–807.
26 B. R. Varlow and D. W. Auckland, Mechanical aspects of electrical treeing in solid insulation, *IEEE Electr. Insul. Mag.*, 1996, **12**, 21–26.
27 B. R. Varlow and D. W. Auckland, The influence of mechanical factors on electrical treeing, *IEEE Trans. Dielectr. Electr. Insul.*, 1998, **5**, 761–766.
28 Q. Yan, H. Xu, X. Cheng and C. Wang, in *2023 3rd International Conference on Energy Engineering and Power Systems (EEPS)*, IEEE, Dali, China, 2023, pp. 214–217.
29 F. Hu, C. Emersic, D. Smith, L. Chen, S. Rowland and L. Cunningham, The Effect of Mechanical Strain on Electrical Tree Development in XLPE, *IEEE Trans. Dielectr. Electr. Insul.*, 2024, **31**, 313–321.
30 B. X. Du, J. G. Su, J. Li and T. Han, Effects of mechanical stress on treeing growth characteristics in HTV silicone rubber, *IEEE Trans. Dielectr. Electr. Insul.*, 2017, **24**, 1547–1556.
31 B. X. Du, J. G. Su and T. Han, Effects of mechanical stretching on electrical treeing characteristics in EPDM, *IEEE Trans. Dielectr. Electr. Insul.*, 2018, **25**, 84–93.
32 B. Du, W. Zhang and H. Liang, Combined Effects of Electrical and Mechanical Stresses on Insulation Breakdown—Part I: Tree Growth of Epoxy Resin, *IEEE Trans. Dielectr. Electr. Insul.*, 2023, **30**, 2362–2369.
33 S. Mita and K. Yahagi, Effect of Elongation on Dielectric Breakdown Strength in Polyethylene, *Jpn. J. Appl. Phys.*, 1975, **14**, 197–201.
34 E. Ildstad and S. T. Hagen, in *Conference Record of the 1992 IEEE International Symposium on Electrical Insulation*, IEEE, Baltimore, MD, USA, 1992, pp. 135–139.
35 Z. Li, F. Dai, Y. Wu and B. Du, Effect of Crystalline Morphology on Electrical Tree Morphology and Growth Characteristics of PP Insulation: From Mesoscopic to Macroscopic, *IEEE Trans. Dielectr. Electr. Insul.*, 2023, **30**, 989–996.
36 B. Du, G. Sun, H. Wang and Z. Li, Effect of Bending Deformation on Electrical Tree Properties of Polypropylene Copolymer and Blend Insulation for HVDC Cables, *IEEE Trans. Dielectr. Electr. Insul.*, 2025, **32**, 789–796.
37 M. A. Fard, M. E. Farrag, S. McMeekin and A. Reid, Electrical Treeing in Cable Insulation under Different HVDC Operational Conditions, *Energies*, 2018, **11**, 2406.
38 *Recommendations for mechanical testing of submarine cables*, ed. CIGRE TB 623, CIGRE, Paris, 2015.
39 X. Chen, Y. Xu, X. Cao, S. Dodd and L. Dissado, Effect of tree channel conductivity on electrical tree shape and breakdown in XLPE cable insulation samples, *IEEE Trans. Dielectr. Electr. Insul.*, 2011, **18**, 847–860.
40 T. A. Ve, H. M. Syvertsen, N. M. Thomsen, M.-H. Ese, E. Kantar and S. Hvidsten, Electrical Treeing in Fluoropolymer Cable Insulation, *IEEE Trans. Dielectr. Electr. Insul.*, 2024, **31**, 1918–1925.
41 M. M. Adnan, T. A. Ve, S. Hvidsten, M.-H. G. Ese, J. Glaum and M.-A. Einarsrud, Electrical Treeing and Partial Discharge Behaviour in Epoxy Nanocomposites with in situ Synthesized SiO_2, *IEEE Trans. Dielectr. Electr. Insul.*, 2023, **30**, 936–945.
42 G. J. Malkin and B. R. Varlow, Electrical treeing in mechanically prestressed insulation, *IEEE Trans. Dielectr. Electr. Insul.*, 2000, **7**, 721–724.
43 A. C. Ferrari, Raman spectroscopy of graphene and graphite: Disorder, electron–phonon coupling, doping and nonadiabatic effects, *Solid State Commun.*, 2007, **143**, 47–57.
44 A. S. Vaughan, S. J. Dodd and S. J. Sutton, A Raman microprobe study of electrical treeing in polyethylene, *J. Mater. Sci.*, 2004, **39**, 181–191.
45 J. Holto and E. Ildstad, in 2010 10th IEEE International Conference on Solid Dielectrics, IEEE, Potsdam, Germany, 2010, pp. 1–4.
46 J. Holto, E. Ildstad and I. Lunde, in *2012 International Conference on High Voltage Engineering and Application*, IEEE, Shanghai, China, 2012, pp. 63–67.
47 A. S. Deshpande, H. A. Mangalvedekar and A. N. Cheeran, Partial discharge analysis using energy patterns, *Int. J. Electr. Power Energy Syst.*, 2013, **53**, 184–195.
48 H. Ichikawa, Y. Suzuoki, T. Mizutani and K. Uchida, in *Proceedings of* 1994 *4th International Conference on Properties and Applications of Dielectric Materials (ICPADM)*, IEEE, Brisbane, Qld., Australia, 1994, vol. 1, pp. 379–382.
49 Z. Lv, S. M. Rowland, S. Chen, H. Zheng and I. Iddrissu, Evolution of partial discharges during early tree propagation in epoxy resin, *IEEE Trans. Dielectr. Electr. Insul.*, 2017, **24**, 2995–3003.
50 J. V. Champion and S. J. Dodd, Simulation of partial discharges in conducting and non-conducting electrical tree structures, *J. Phys. D: Appl. Phys.*, 2001, **34**, 1235–1242.
51 S. J. Dodd, N. M. Chalashkanov and J. C. Fothergill, in *2010 10th IEEE International Conference on Solid Dielectrics*, IEEE, Potsdam, Germany, 2010, pp. 1–4.
52 J. P. Torres, P. M. Frontini, M. Machado and Z. Major, Deformation and failure of semicrystalline polymers under dynamic tensile and biaxial impact loading, *Int. J. Impact Eng.*, 2016, **98**, 52–61.
53 A. Peschot, N. Bonifaci, O. Lesaint, C. Valadares and C. Poulain, Deviations from the Paschen's law at short gap distances from 100 nm to 10 μ m in air and nitrogen, *Appl. Phys. Lett.*, 2014, **105**, 123109.
54 J. M. Rodríguez-Serna, R. Albarracín-Sánchez, M. Dong and M. Ren, Computer Simulation of Partial Discharges in Voids inside Epoxy Resins Using Three-Capacitance and Analytical Models, *Polymers*, 2020, **12**, 77.
55 I. Iddrissu, Z. Lv and S. M. Rowland, in *2016 IEEE* International Conference on Dielectrics (ICD), IEEE, Montpellier, France, 2016, pp. 728–731.
56 S. Rastogi, A. B. Spoelstra, J. G. P. Goossens and P. J. Lemstra, Chain Mobility in Polymer Systems: on the Borderline between Solid and Melt. 1. Lamellar Doubling during Annealing of Polyethylene, *Macromolecules*, 1997, **30**, 7880–7889.

57 K. Wu, Y. Suzuoki, T. Mizutani and H. Xie, A novel physical model for partial discharge in narrow channels, *IEEE Trans. Dielectr. Electr. Insul.*, 1999, **6**, 181–190.
58 L. Zhou, J. Cai, Q. Qiu, L. Guo and R. Cheng, Temperature–dependent effect of gas pressure on electrical tree in XLPE cable, *IET Sci., Meas. Technol.*, 2019, **13**, 678–683.
59 N. H. Aziz, V. M. Catterson, S. M. Rowland and S. Bahadoorsingh, Analysis of partial discharge features as prognostic indicators of electrical treeing, *IEEE Trans. Dielectr. Electr. Insul.*, 2017, **24**, 129–136.
60 S. Abdul Madhar, P. Mraz, A. Rodrigo Mor and R. Ross, Physical interpretation of the floating electrode defect patterns under AC and DC stress conditions, *Int. J. Electr. Power Energy Syst.*, 2020, **118**, 105733.
61 M. Camalov, F. Akin, A. Hashimov, O. Arikan, A. Orucov and M. Guliyev, The Degradation Analysis of XLPE Materials Under Thermal Aging: A Comprehensive Study Through Partial Discharge Measurements and Structural Characterization Techniques, *Trans. Electr. Electron. Mater.*, 2024, **25**, 494–506.